Free-radical Probes for Functional in vivo EPR Imaging

S. Subramanian and M. C. Krishna
Radiation Biology Branch, Center for Cancer Research, NCI, National Cancer Institute,
National Institutes of Health, Bethesda, MD 20892, USA

Abstract

Electron paramagnetic resonance imaging (EPRI) is one of the recent functional imaging modalities that can provide valuable in vivo physiological information on its own merit and aids as a complimentary imaging technique to MRI and PET of tissues especially with respect to in vivo pO_2 (oxygen partial pressure), redox status and pharmacology. EPR imaging mainly deals with the measurement of distribution and in vivo dynamics and redox changes using special non-toxic paramagnetic spin probes that can be infused into the object of investigation. These spin probes should be characterized by simple EPR spectra, preferably with narrow EPR lines. The line width should be reversibly sensitive to the concentration of in vivo pO_2 with a linear dependence. Several non-toxic paramagnetic probes, some particulate and insoluble and others water-soluble and infusible (by intravenous or intramuscular injection) have been developed which can be effectively used to quantitatively assess tissue redox status, and tumor hypoxia. Quantitative assessment of the redox status of tissue in vivo is important in investigating oxidative stress, and that of tissue pO_2 is very important in radiation oncology. Other areas in which EPR imaging and oxymetry may help are in the investigation of tumor-angiogenesis, wound healing, oxygenation of tumor tissue by the ingestion of oxygen-rich gases, etc. The correct choice of the spin probe will depend on the modality of measurement (whether by CW or time-domain EPR imaging) and the particular physiology interrogated. Examples of the available spin probes and some EPR imaging applications employing them are presented.

Key words: Free radicals, spin probes, EPR imaging, Oxymetry, Oxidative stress, tumor hypoxia, Nitric oxide, spin trapping, functional imaging, nitroxides

1. INTRODUCTION

Imaging science which is a truly multidisciplinary approach involving chemists, physicists, mathematicians, computer scientists and biologists is very important in the diagnosis of diseases and in recent years, imaging at the molecular level has become very essential in understanding of biochemical and molecular mechanisms. Imaging techniques use almost the entire range of the electromagnetic spectrum from γ-rays to very low energy radiofrequency radiation. In the high energy end one uses γ-radiography in imaging internal structure of heavy metal welds and refractory materials where ordinary light cannot penetrate. X-rays have been traditionally used in diagnostic radiology as the only method until other methods were discovered. These include computerized axial tomography (CAT), infrared, fluorescence, magnetic resonance (MRI), ultrasound etc. Most of the imaging methods that are used in vivo not only provide anatomical details but additional functional information as well. Among all this, MRI occupies a unique position in diagnostic radiology capable of locating tumors and malignancy deep inside tissue, functional imaging of the brain, blood flow and blood volume, diffusion tensor of water and a host of other possibilities[1-3]. A relatively recent mode of imaging employs the technique of Electron Paramagnetic Resonance, EPR, which closely resembles MRI, but uses as its probe molecules with unpaired electrons, the so-called free radicals. Electron Paramagnetic Resonance Spectroscopy and Imaging (EPR and EPRI) are identical to Nuclear Magnetic Resonance Spectroscopy and Imaging (NMR and MRI). While NMR deals with the frequency of precession of magnetic nuclei, protons in particular, in a magnetic field, EPR deals with that of the unpaired electrons[4-6]. The magnetic moment of the electron is nearly three orders of magnitude larger. Traditionally EPR spectroscopy used to be carried out at MW frequencies (9 - 35 GHz range) corresponding to magnetic fields in the range 0.3 to 1.2 Tesla)), but at these frequencies the penetration in biological medium is less than an mm. Hence, in vivo EPR spectroscopy deep in tissue requires frequencies under a GHz. Most small animal imaging to date has been carried out at frequencies under 500 MHz. Before we review the applications of in vivo EPR spectroscopy and imaging, it is essential to consider the importance of free radicals in biology and the role EPR imaging can play in our understanding physiological processes involving endogenous as well as externally introduced free radical probes.

In chemistry, free radicals are molecular or atomic species which have one or more unpaired electrons with the so-called open-shell configuration. Because systems with unpaired electrons are unstable (there are, of course, exceptions, vide infra), free radicals are very reactive, and their neutral charge (there are charged free radicals as well) endows them with reaction patterns that are quite different from reactivity of charged species. Free radicals occur in combustion, electrochemical, chemical and enzymatic redox reactions as intermediates. They occur in gas phase reactions in the atmosphere. More importantly, many free radicals are implicated in biochemical and human physiological processes. The first organic free radical, triphenylmethyl, was identified and reported by Moses Gomberg[7] in1900, who, apparently wanted to "reserve the field" for himself. For example the reactive oxygen species superoxide, O_2^- and nitrogen species, nitric oxide, NO are free radicals that are involved in oxidative stress and vascular control. A number of reactions that involve lipid peroxidation involve toxic free radical intermediates[8, 9]. Several bioactive molecules undergo interesting redox reations involving one or many electron transfers, often through free radical intermediates. Free radicals play an important role in a number of biological processes, some of which are necessary for life, such as the intracellular killing of bacteria by neutrophil granulocytes. Free radicals have also been implicated in many cell signalling processes. Superoxide (O_2^-) and hydroxyl (OH) radicals which are derived from molecular oxygen under reducing conditions are highly reactive and can participate in many side reactions resulting in cell damage. Intercalation of free radicals with DNA has been advanced as reasons for mutations leading to many forms of cancer. Symptoms of aging have also been attributed to oxidation of many of the chemicals making up the body leading to the so-called oxidative stress[10, 11]. There are many more physiological processes involving the occurrence and action of free radicals that are continued to be dicovered. Although many free radicals occur in living systems, the concentration of these endogenous species is rather low, and often most in vivo radicals are short-lived. EPR imaging employing free radicals will therefore entail the introduction of free radicals into the subject of imaging.

We can classify the various free radical probes that can be used for in vivo spectroscopy and imaging into particulate oxygen sensors, carbon chars, scores of stable five and six membered ring nitroxides, organic free radicals derived from triarylmethyl (TAM), etc., which can be introduced into the living system to interrogate specific pathophysiology[12]. It is also possible to employ spin traps as 'precursor' spin probes[13]. Spin trapping is a procedure to study transient free radicals that are usually unstable and have short half-lives by allowing them to react with a the so-called spin-trapping agent which results in the formation of much stabler free radicals known as spin-adducts. This novel procedure allows unstable radicals to be identified and studied by both EPR spectroscopy and imaging. The most widely used spin trap is PBN, (N-tert-butyl-alpha-phenyl nitrone) which has been shown to extend the lives of many short-lived free radicals in vivo and in vitro. These spin traps can also help in assessing the efficiency of anti-oxidants that fix and remove unwanted reactive oxygen species, before and after treatment[14-16]. There also spin labels, that are stable compounds with an unpaired electron, usually localized near a nitrogen nucleus that can bind to a macromolecule at specific sites[17]. Once the labeling is done, the hyperfine pattern of the EPR spectrum from the spin label will have spectral patterns that can provide, after careful analysis and simulation, critical information of the nature of the specific location and its dynamics. Double spin labeling of large proteins at specific sites can provide further information on the distance between the labeled sites and their dynamics leading to three dimensional structural information of the macromolecules[18, 19]. There are indeed a large number of synthetic spin traps and spin labels designed for addressing specific molecular structural investigations and the subject is beyond the scope of this article.

We will not be dealing with the vast subject of free radicals for which many articles and monographs are available[20, 21]. Rather we shall confine ourselves with some of the spin probes that will be of use in EPR imaging. Obviously, we cannot be exhaustive in our treatment of the subject, witch is a fast growing field. In the following we first give a brief description of the EPR spectroscopy and imaging methodology followed by the various bio-compatible spin probes that have been used for in vivo experiments. Also outlined are some of the specific applications where EPR imaging and spectroscopy can provide useful functional physiological information.

2, PHENOMENOLOGICAL DESCRIPTION OF EPR SPECTROSCOPY AND IMAGING

Electron Paramagnetic Resonance (EPR) and Nuclear Magnetic Resonance (NMR) are two major spectroscopic phenomena discovered during the middle of the last century[4-6]. These two techniques are based respectively on the magnetic dipole moment of the electron and that of nuclei with non-zero spin, and monitor their precessional

frequencies when these are placed in a uniform DC magnetic field, known as the Zeeman field. The magnetic moments of nuclei are nearly three orders of magnitude smaller than that of the electron.

The unpaired electron has a spin $S = \frac{1}{2}$ and has two energy levels in an externally applied field. For a field of 1 Tesla (10,000 Gauss), the separation in energy between the two levels correspond to a frequency ν of 28.02 GHz. The relative population of the two levels are governed by Boltzmann statistics, there being a slight excess population of spins in the lower level. The net magnetization from an ensemble of electrons experiences a torque from the external field and precesses with a circular frequency $2\pi\nu$, known as the Larmor frequency. A circularly polarized source of electromagnetic radiation at the Larmor frequency resonates with the spin system thereby causing exchange between the spins and the source to bring about resonance absorption that tend to reduce the population difference between the levels. The system reverts back to its normal equilibrium population via two first order processes known as the spin-lattice and spin-spin relaxation times (T_1 and T_2). In simple terms, the phenomenon of resonance absorption brings about a coherence of magnetization in the plane perpendicular to the Zeeman field axis, which, left to itself, gradually dephases and ultimately becomes zero when all the magnetization vectors have become fully randomized. This process, known as transverse relaxation, characterized by a first order time constant T_2 (spin-spin relaxation or phase memory time), is an energy-conserving process, there being only exchange of energy among the spins brought about by magnetic interactions. When the resonance phenomenon is accomplished by a continuous wave (CW) approach (sweep of the magnetic field keeping the frequency constant, or *vice versa*) a resonance absorption with a Lorentzian line shape results, whose width is related to the above-mentioned relaxation time. The full width of the resonance absorption at half maximum height (FWHM) is equal to $(\pi T_2)^{-1}$. If one tries to accomplish the resonance condition by applying a pulse of electromagnetic radiation, the time response of the system, which is simply the inverse Fourier transform of the resonance absorption that would be obtained in the CW experiment, is a damped exponentially decaying sinusoidal signal with a time constant characterized by T_2. In EPR the line widths are on the order of tens of mG to several Gauss depending on the particular paramagnetic system. The transverse relaxation time and hence the line width of many paramagnetic probes are affected by the presence of molecular oxygen. This is because, molecular oxygen is paramagnetic with two unpaired electron per molecule, and hence can interact with free radicals via direct magnetic dipolar or Heisenberg exchange interaction[22] that causes a broadening of the line width, and in most cases, this broadening is a linear function of the in vivo partial pressure of oxygen, pO_2[23-25]. This phenomenon is a unique property of most free radicals that can be monitored by EPR and helps to perform quantitative oxymetry in living systems. No other method is capable of providing such a spatial distribution of pO_2 in a non-invasive manner.

The absorption of energy from the radiation source creates non-equilibrium population for the ensemble of spins, and once the radiation is shut off, the system reverts back to its Boltzmann equilibrium via another first order process known as the spin-lattice relaxation or longitudinal relaxation, T_1. This is an energy non-conserving process, there being exchange of energy between the system and its surrounding 'lattice'. The magnitudes of T_1 and T_2 depend on the efficiency with which the spins are coupled to each other and the surroundings and depend on the temperature, viscosity of the medium, rigidity of the lattice, and other dynamical properties of the system, such as the molecular reorientation correlation time, presence of other magnetic impurities, etc. The relaxation times T_1 and T_2 are on the order of ns-µs in solution or liquid state. In rigid solids, T_1 can be much longer and T_2 is very short, and at all situations $T_2 \leq T_1$.

The single resonance absorption of the unpaired electron can acquire additional fine structure by interaction with any associated magnetic nuclei in the molecule known as the hyperfine splitting. For interaction with the ^{14}N nucleus, for example in a nitroxide free radical, the EPR spectrum will consist of a triplet of equally spaced hyperfine lines (the naturally occurring ^{14}N nucleus has a spin $I = 1$, and it has $2I+1$ equally probable orientations in an external field leading to three equally intense, equally spaced hyperfine lines). In systems with multiple interacting magnetic nuclei, the spectra can be quite complicated due to many hyperfine lines some of which may overlap with each other. A few simulated EPR spectra are shown in Fig.1.

In CW EPR, the spectra are obtained by monitoring the absorption of MW or RF radiation from a resonant cavity as a function of sweeping the magnetic field. Instead of directly detecting the absorption, what is usually done is to modulate the Zeeman field by a low frequency AC field, and detect the EPR signal using a lock-in amplifier and phase-sensitive detector, leading to a first derivative of absorption (dI/dB) that will appear as a Lorentzian derivative. The

peak-to-peak width of this Lorentzian derivative (ΔB_{pp}) is related to the FWHM of the corresponding absorption by ΔB_{pp} = FWHM $/\sqrt{3}$. Detailed descriptions of the working of CW EPR spectrometers are available in the literature [26-28]
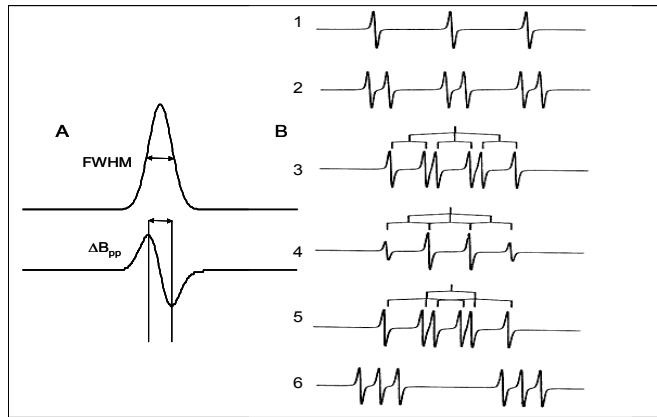

Fig.1 **A**. A typical single line EPR spectrum. The Lorentzian absorption and the corresponding first derivative line shapes are shown. $\Delta B_{pp} = (1/\sqrt{3})*$FWHM. **B**. Computer-simulated ESR spectra of nitroxides with and without doublet splitting. (1) ESR triplet spectrum due to a nitroxide with only a triplet hyperfine from nitrogen nucleus. (2) For a nitroxide interacting with a single spin ½ nucleus (proton) with A_H much less than A_N. (3) Spectrum for nitroxide when A_H approaches the value of A_N (4) The spectrum of a nitroxide with equal A_N and A_H (5) Here A_H has just exceeded A_N (6) In his spectrum the nitrogen hyperfine coupling is much less (nearly 1/8) than that from an interacting nucleus with spin ½.

In pulsed EPR one subjects the spin system in a resonant cavity by an intense narrow(~100 ns) RF pulse of 100-200W power so that the Zeeman magnetization is rotated into the transverse plane, and the resulting rotating magnetization from the spin ensemble is acquired by a fast digitizer after suitable amplification. The resulting response (known as the free induction decay, FID) which lasts only for a few microseconds are to be acquired using a fast digitizer and subjected to Fourier transform, resulting in a spectrum that would be identical to the Lorentzian absorption that would be obtained by a CW mode of detection. Since the impulse response of the spin system depends on the transverse relaxation time T_2^*, only systems with very narrow spectral line width (<500 mG, and concomitantly a longer transverse relaxation time, $T_2 > 300$ ns) are amenable to be detected in low frequency pulsed EPR. This, of course, limits the range of available spin probes for pulsed EPR spectroscopy and imaging, while CW EPR has no specific limitation on the probe line width. Details of pulsed EPR spectrometers operating at Radiofrequency regions have already been published by us and others[29-32]. It should be emphasized here that both CW and Pulsed spectrometers operating at or below 750 MHz are required for investigating free radicals deep in tissue, while higher frequencies are acceptable only for surface applications.

As far as EPR imaging is concerned, both CW and time-domain methods have been developed for applications to small animals and excised tissue. In CW EPR imaging[12, 33, 34] one obtains the spectrum in presence of linear magnetic field gradients just as was done in the early development of NMR imaging[35]. This results in encoding the spatial distribution of spins in terms of projections along specific directions, just as in X-ray CT. These projections are subject to filtered back-projection to generate the image of the spin distribution in 1, 2 and 3D. In the case of time-domain EPR imaging one can use the projections obtained after FT of the FIDs collected in presence of gradients for the back-projection reconstruction of the images. It is also possible to subject each single time point in the FID to pure phase encoding and then collect the amplitude modulation this will generate as a function of rastering the gradients in one, two or three dimensions. The resulting n-dimensional k-space upon FT can provide the image. In this so-called single point imaging (SPI) modality[36-40], a given constant point has only spatial information. Each time point will generate an image and the field of view is governed by gradient increments and the delay from the pulse. Images derived from consecutive time points will have a zoom-in effect proportional to the delay. Detailed descriptions of the time-domain EPR imaging using back-projection as well as SPI have already been published[32, 40]

Spatially resolved spectroscopic information can be obtained by the so-called spectral-spatial imaging[41-45]. Only then we can get spatially resolved functional information. A cursory description is given here. This is based on the fact that at zero gradient the spectrum has no spatial information, whereas at infinite gradient there will be only pure spatial information. In other words, in a pseudo spectral-spatial domain spectral and spatial axes will be orthogonal to each other. At finite gradients therefore the projections correspond to a specific viewing angle, known as the pseudo viewing angle α. In this modality spatial encoding is done just as in conventional tomography, but an additional pseudo spectral

dimension is generated by generating each of the projections in presence of systematically increasing gradients. Rescaling the spatial window at higher gradients to the zero-gradient spectral window will correspond to a pseudo viewing angle α given by,

$$\tan\alpha = (spatial\,window\,/\,specrtal\,window)*gradient\,magnitude \qquad [1]$$

Pseudo angles close to α = 90 is impractical and we will have some missing angles. The rescaled projections can be subjected to filtered back-projection in which, along the spectral axis, we can get spatially resolved pure spectral information which can be used to infer physiological information such as oxygen concentration, after proper calibration. Spectral spatial imaging has been implemented in CW EPR imaging by several researchers where one can get a more detailed description than given here[41-45]. The same procedure can be adopted in time-domain spectral spatial EPR imaging, the only difference being that instead of obtaining the projections directly from a field sweep, they are generated from the FIDs obtained under the gradients. A much more efficient way of performing spectral spatial imaging is unique to the Single Point imaging scheme mentioned above. Here the images processed from the various time points from an FID. After scaling to identical field of view, the images will have their pixel intensities, in successive corresponding pixels, governed by the transverse relaxation time T_2^* which has also the same information as the line width, augmented by additional broadening from gradients and magnetic susceptibility. One interesting fact is that since the FIDs are collected within microseconds with a fast digitizer, we have literally hundreds of images which are exponentially weighted by the transverse decay time in each pixel. A careful analysis of the sequence of images can provide spectral spatial information by way of providing pixel-wise T_2^* which can be used to derive quantitative information on in vivo pO_2. Detailed descriptions of spectral spatial imaging using the SPI modality both in EPR imaging and solid state MRI have already been published[32, 46, 47].

3. SPIN PROBES FOR IN VIVO EPR

3.1 Particulate spin probes baes on carbonchars

Particulate spin probes that are used for in vivo RPR studies are those that can be surgically implanted in specific anatomical locations for monitoring the immediately surrounding tissues in vivo. They are good to provide information from a point location. Many of these particulate spin probes are biologically inert, and can be left in a specific location for repeated monitoring as a function of treatment. Chronologically carbon chars were the first ones to be identified to have a reversible line width effect depending on the partial pressure of oxygen[48-50]. The measurement of oxygen partial pressure based on the in vivo line width of paramagnetic systems such as carbon chars was termed EPR oxymetry. These carbon chars have a wide variation in their oxygen-free line width and oxygen relaxivity (linewidth change per unit oxygen concentration) depending on their source material, and their preparation[23, 51-53]. Carbonaceous materials such as wood, cotton, sugars, etc. under controlled thermal treatment yield the chars, with a good concentration of unpaired electrons (10^{18}-10^{19} spins/gm) . Their stability and oxygen sensitivity critically depend on the exact treatment history. They can be powdered and sieved to narrow range of sizes since the parameters such as EPR line width, bio-stability, oxygen relaxivity etc., depend critically on the particle size. They can be implanted either as such are encapsulated in gas permeable coatings, such as cellulose nitrate before implantation. Because of the difficulty in producing chars with identical properties, for quantitative application, they require a batch-wise calibration of line width versus pO_2. Nevertheless, they are quite useful as non-toxic oxymetric probes.

Fusinite is another carbon based spin probe that was used in early oxymetric studies by CW EPR[54]. Coal is a rock formed by geological processes and is composed of a number of distinct organic entities called macerals. Macerals are derived from plant material that has been strongly altered and degraded in the peat stage of coal formation and fossil charcoal is the inertinite maceral, known as fusinite. Fusinite gives a single EPR line of 1Gauss line width in the absence of oxygen which increases to 4Gauss at 20% oxygen. The increase, although monotonic and reproducible, is not linear. This non-linearity can be due to different mechanisms such as multi-site electron exchange, g-strain broadening, adsorption of oxygen, etc.

Another form of chars, namely India ink, known to have existed well before 1200 B.C., consists of emulsified carbon particles in a base of vegetable oil and gelatin. India ink gives a strong EPR line which shows very good oxygen

sensitivity. It is quite non-toxic proven by its use in tattoos from time immemorial and, as such, could be easily accepted in a clinical setting**. The line width dependence on oxygen is very high, so much so that the intensity of the EPR line will rapidly decease above 20 torr. As such it would be useful to accurately monitor low pO_2. It is especially suitable for monitoring oxygen concentration in skin, and to assess oxygen in the extremities of diabetic patients to evaluate peripheral vascular diseases and in wound healing using topical resonators such as surface coils. EPR studies in animal tumors have also been reported using India ink[53, 55-57].

3.2 Lithium- phthalocyanine/naphthalocyaninecrystals

One of the most widely used particulate EPR oxymetric probe is Lithium phthalocynaine, LiPc obtained as a result of electrochemical oxidation of the diamagnetic dilithium phtahlocyanine, Li2Pc. The structure of LiPc is shown in Fig. 2. LiPc can be synthesized by procedures similar to those reported earlier[24, 25, 58, 59]. Electrolysis is performed under air and at constant potential resulting in pO_2-sensitive crystals. A solution of Li2Pc is oxidized to LiPc in acetonitrile solution using tetrethylamminaium perchlorate as the supporting electrolyte, at a controlled potential using an voltammograph in an electrochemical cell using Pt electrodes. Platinum electrodes are used for both as the working and auxiliary electrodes. The auxiliary electrode is a coiled Pt wire inside a fritted glass, while the working electrode is either a Pt gauze, a Pt coil, or a Pt coiled coil. The value of the oxidation potential is critical and, for example, at 0.4V against Ag1/AgCl(s) electrode crystalline LiPc separates out that can be filtered, washed and dried. Detailed work on the electrochemical preparation, the nature of the crystals obtained, and their oxygen sensitivity, mechanism of oxygen broadening, etc., have been reported[24, 25]. The oxygen sensitivity of the LiPc particles is strongly dependent on the size of individual crystals. By careful control of the electrolytic oxidation parameters one can obtain crystals of more or less uniform size with good reproducible oxygen sensitivity. Among all particulate spin probes. LiPc perhaps has the best linear response to oxygen partial pressure. Each batch of crystals, however, has to be calibrated for their oxygen relaxivity (line broadening), and measurements have to be carried out under very low MW/RF power to avoid saturation, and low modulation amplitude to avoid modulation broadening.
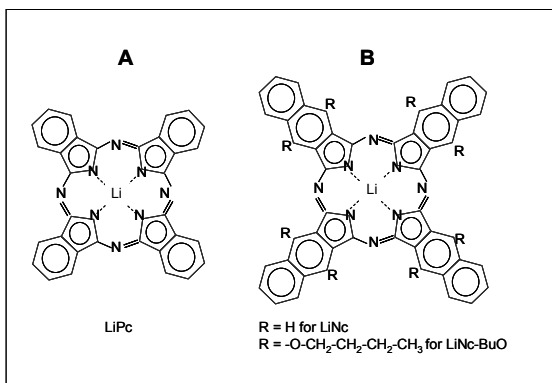

Fig. 2. The molecular structures of Lithium phthalocynaine, Lithium naphthalocyanine and Lithium octa-butoxy naphthalocyanine.
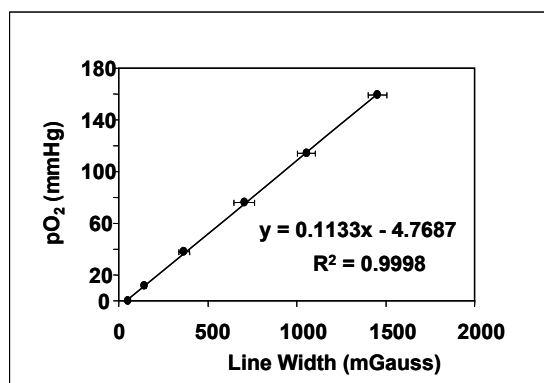
Fig. 3. Plot of the partial pressure of oxygen versus the Lorentzian peak-to-peak line width of LiPc from 750 MHz CW EPR measurement. LiPc crystals were equilibrated in a flowing gas mixture of appropriate ratios of nitrogen and oxygen for 30 minutes before each measurement.

Fig.3 shows a graph of oxygen partial pressure (pO2) versus peak-to-peak derivative line width of LiPc carried out at 700 MHz in a home-built CW spectrometer. The linearity and the good dispersion in oxygen sensitivity makes this probe ideal for in vivo oxymetry of internal organs, where one can surgically implant these crystals, and make repeated measurements. But for the invasive placement, LiPC based EPR spectroscopy is one of the most quantitative and reliable way to perform site-specific oxymetry. Liu et al[60] have reported very interesting applications of LiPc based EPR oxymetry at L-band (1.2 GHz) in investigating myocardial pO_2 in rats as a function of the oxygen content of the respiratory gas, in the rat kidney cortex before and after aortic ligation, and in rat brain in anesthetized and unanesthetized conditions. LiPc particles, in most tissues, remain stable without undergoing any bio-degradation, although in certain locations such as skeletal muscles, due to deposition of minerals, the oxygen permeability can get

reduced leading to impaired oxygen sensitivity. Nevertheless many in vivo experiments have shown that the crystals remain unaffected and can report on oxygenation status for at least 5-6 weeks of repeated measurements.

We have carried out CW EPR experiments in mice[61, 62] to investigate absolute partial pressure of oxygen (pO$_2$) in the mammary gland pad and femoral muscle of female mice using EPR oxymetry at 700 MHz. The pO$_2$ values in the tissue became stable 2 weeks after implantation of LiPc crystals. The pO$_2$ level was found to be higher in the femoral muscle than in the mammary tissue. However, the pO$_2$ values showed a strong dependence on the core body temperature of the mice. The pO$_2$ values were responsive to Carbogen (95% O$_2$, 5% CO$_2$) breathing even six to seven weeks after the implantation of LiPc. The LiPc linewidth was also sensitive to changes in the blood supply even 60 days after implantation of the crystals. These results are summarized in Fig.4. This study clearly validates the use of LiPc crystals for long-term non-invasive repetitive assessment of pO$_2$ levels in vivo by EPR.
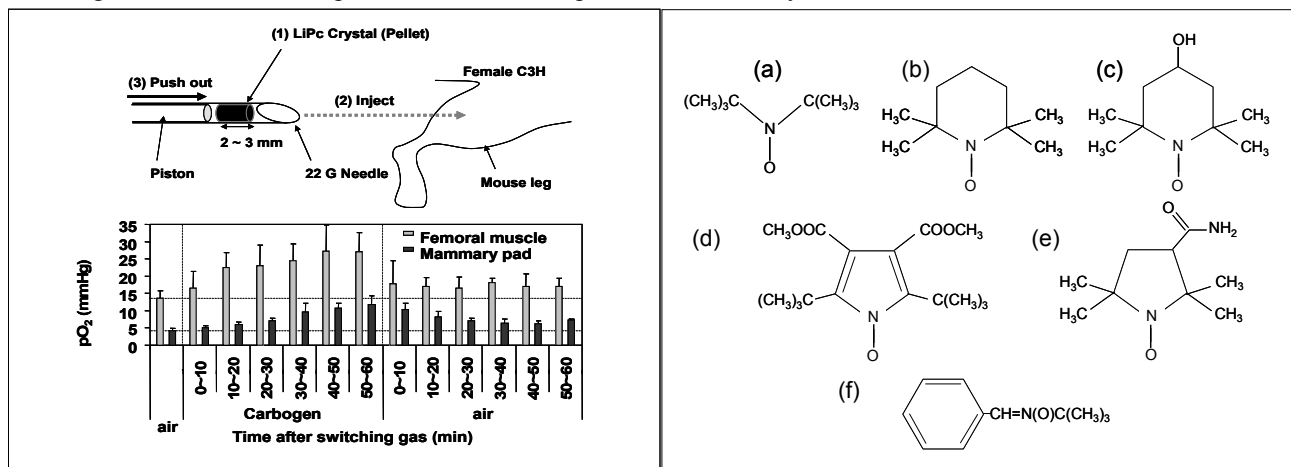

Fig. 3 .**Top:** A cartoon describing the implanatation of LiPc crystals in the muscle tissue of a mice. **Bottom:** The time course of the in vivo oxygen partial pressure in the femoral muscle and the mammary pad of a C3H mouse as a function of the breathing air or Carbogen . See for text for details.

Fig.4 Structure of some common nitroxides (a) D-tertiary butyl nitroxide b. Piperidine N-oxyl (TEMPO) c. 4-hydroxy TEMPO, TEMPOL d. Pyrrol N-oxyl   e. 3-carboxamido-2,2,5,5-tetramethylpyrrolidine-*N*-oxyl (3-carbamoyl-proxyl) [3-CP] f. N-tert.-butyl-phenylnitrone (PBN).

Two other Li-based based derivatives, namely lithium naphthalocyanine (LiNc)[63,64] and lithium lithium octabutoxynaphthalocyanine (LiNc-BuO) [65] have been reported which also are excellent particulate probes for oxymetry (Fig.2). It has been recently shown that the LiNc-BuO crystals are also useful for estimating nitric oxide, NO which also produces a line broadening linearly with NO concentration[66].

3.3 Soluble spin probes based on nitroxides

Nitroxides are compounds of the general formula R$_2$NO (or RR'NO) with the free electron localized on the $\pi*$ orbitals of nitrogen and oxygen, with the nitrogen atom linked two carbon atom of R/R'. More commonly the NO group is linked to two carbons which are part of five or six membered cyclic compounds. If the carbon adjacent to the nitrogen has two methyl groups, then steric factors endow additional stability to the nitorxide. Stable nitroxide free radicals have found a wide range of applications in biology and medicine. These compounds have been used to monitor intracellular redox reactions, oxygen concentration and pH, and as contrast agents in magnetic resonance imaging, and as probes in EPR imaging[67-69]. Persistent nitroxide adducts resulting from reaction of a precursor nitrone (spin trap) with transient free radical species have been used to detect, characterize, and quantitate the production of free radicals in various in vitro and in vivo model systems[70]. The cellular and in vivo pharmacology of stable nitroxides and the spin adduct nitroxides has been investigated in detail[71, 72]. The six-membered saturated ring nitroxides known as piperdine nitroxides are called Tempo derivatives. The five membered ring nitroxides are derived from pyrrole. These nitroxides can be functionalized by various substitutions such as hydroxyl, carboxyl or ester groups. It should be mentioned here that there are a number of diamagnetic nitrone and nitroso compounds which are precursors of nitroxides. These

nitrones and nitroso compouns act as spin traps for unstable radicals resulting in some what more stable nitroxde spin adducts. All nitroxides basically give a major triplet EPR spectrum with a nitrogen hyperfine coupling in the range 15-17 Gauss. In solution of low viscosity the lines are Lorentzian in shape. Superhyperfine structure from other magnetic nuclei in the molecule (especially protons of hydrogen atoms) is often resolved, and the hyperfine pattern is often used as a handle to identify the transient free radicals generated in spin trapping experiments[13]. Perdeuteration of the nitroxides can lead to very narrow EPR lines making them suitable for high resolution EPR imaging. The structure of some representative nitroxides that are used in biochemical and physiological studies are given in 5

Previous studies have shown that the stable five-membered nitroxide, 2-ethyl-2,5,5-trimethyl-3-oxazolidine-1-oxyl (OXANO), is a cell-permeable, nontoxic, catalyst of superoxide (O_2^-) dismutation[73]. Cellular studies have also established this and other stable nitroxides can act as protective agents for cells subjected to oxidative stress induced by agents such as O_2^-, H_2O_2, organic hydroperoxides, and ionizing radiation[74]. These initial studies led to the synthesis and screening of various five- and six-membered nitroxides to explore their efficiency as superoxide dismutase (SOD) mimics and the degree of protection they can provide against oxidative damage in mammalian cells. The lipophilic piperidinyl nitroxide 2,2,6,6-tetramethylpiperidine-1-oxyl (Tempo) ameliorates post-ischemic reperfusion injury[74], and stable nitroxides have been identified as a new class of non-thiol radioprotectors in vitro[75]. A number of mechanisms for cytoprotection have been advanced; they include oxidation of reduced transition metal ions, detoxification of intracellular radicals such as alkyl, alkoxyl, and alkylperoxyl radicals[76, 77], and direct catalytic removal of O_2^- by dismutation.

Nitroxides are, therefore, ideal spin probes for assessing tumor redox status. The redox status of cells and tissue are governed by several factors including perfusion, degree of oxygenation, levels of antioxidants, and a network of enzymatic systems[78]. Quite a number of intracellular molecules such as glutathione (GSH), thioredoxins, NADPH, flavins, ascorbate, and others control the overall redox status in tissues[78]. Oxidative or reductive stress and alterations in the levels of endogenous/exogenous antioxidants can cause an imbalance in the redox homeostasis of the cells. The cells then revert to the normal redox status by mounting a stress response using various signaling pathways and enzymatic systems. Tumor cells are known to have significant alterations in the redox status compared to normal pathology. The tumor redox status is an important determinant in the response of the tumor to certain chemotherapeutic agents, radiation[79] and bio-reductive hypoxic cell cytotoxins[80]. Therefore, a noninvasive assessment of such information will be useful for tumor treatment planning. Magnetic resonance spectroscopy and positron emission tomography (PET) are two radiologic methods that are capable of providing such information using suitable endogenous probes. EPR imaging has also been developed to provide such information in small animals and potentially in humans. For this, we have to have redox-sensitive probes that can be introduced into the living system, and nitroxides are just the right agents. This is because (a) nitroxide radicals participate in redox-reactions where the nitroxides (paramagnetic, EPR detectable) are reduced to the corresponding hydroxylamines (diamagnetic, EPR silent) and the hydroxylamine can undergo re-oxidation back to the nitroxide[81] and (b) in cells nitroxides undergo reduction to the corresponding hydroxylamines more efficiently under hypoxic conditions than under aerobic conditions via intracellular enzymatic processes[71] When either a nitroxides or the corresponding hydroxylamine is administered in vivo, The level of the nitroxide detectable in vivo remains the same independent of whether the nitroxide or the hydroxylamine is administered because of rapid equilibrium is established between the levels of nitroxide and hydroxylamine. Based on this observation several stable nitroxides have been used as in vivo probes for EPR spectroscopy and imaging experiments to non-invasively obtain tissue/tumor redox status[40, 82-84].

An example of an EPR imaging based assessment of tissue redox status in a mouse model of RIF -1 (radiation induced fibrosarcoma) tumor is outlined below and depicted in Fig.6 Female C3H mice were used. The mice were injected subcutaneously in their right hind leg with a single cell suspension of RIF-1 tumor cells (10^6 cells in 0.1 ml) in PBS and the tumors were allowed to grow to a size of about 8-10 mm in diameter. Mice were anesthetized by and their tail vein was cannulated with a heparin-filled 30-gauge catheter for infusion of the nitroxide probes. 200 μL of a 300 mM solution of the diamagnetic nitroxide 3-CP (3-carbamoyl-2,2,5,5- tetramethylpyrrolidine-n-oxyl, or 3 carbamoyl pro-xyl) in saline was infused before EPR measurement. Using a surface coil resonator placed over the tumor leg EPR images were collected at CW L-band using angular sampling and filtered back projection[85]. A time sequence of 2D images from the tumor shows the heterogeneity of spin distribution, and a rapid reduction in intensities brought about by the reducing environment of the tumor, particularly due to tissue hypoxia, as well as pharmacokinetic clearance (Fig.6A). It is possible to follow the pixel-wise decay of the image intensity and to derive a rate constant for reduction

of the 3CP assuming first order kinetics.(Fig.6B). This is evident by comparison with the much lower rate of nitroxide reduction in normal muscle tissue, which is relatively well oxygenated, although other factors may be involved in the tumor due to its very different physiology. Thiols such as intracellular glutathione and protein thiols play an important role in maintaining the cellular redox status. Although nitroxides do not react with thiols, in microsomal preparations, thiol-containing biomolecules have been shown to play a significant role in the bioreduction of nitroxides[86] Non-invasive assessment of tissue redox status in intact biological organs is important.   Depleting the GSH levels by using specific inhibitors of its synthesis such as L-buthionine-S,R-sulfoximine (BSO) and monitoring the pharmacokinetics of redox sensitive nitroxide probes in both normal as well as tumor tissue should delineate the role of thiols in modulating tissue redox state. Mice treated with BSO, a glutathione depleting agent, showed an overall decrease in the magnitude as well as distribution of reducing equivalents in the tumor (6A, bottom row). This prototype experiment   demonstrates that the redox mapping method using nitroxides by EPRI is a noninvasive means of obtaining spatial and time-resolved pharmacokinetics information, which may be important in the understanding tumor physiology and therapy. Apart from being redox sensitive EPR probes, infusible nitroxides and nitroxide labeled drugs can also be used to follow drug delivery and its pharmacokinetic profile. Extensive work in ths area have been reported by Mader and Gallez[87].
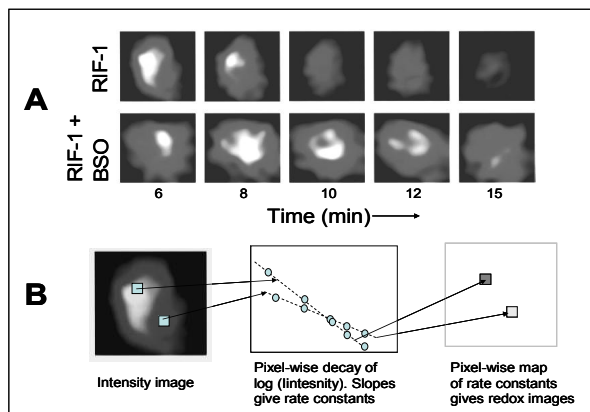

Fig.6 **A**. **Top row**:EPR images from RIF-1 tumor showing fast reduction due to the reducing environment. **Bottom row**. Inhibition of reduction due to the injection of BSO. **B**. Schematic of following pixel-wise decay and generating redox map of decay constants.
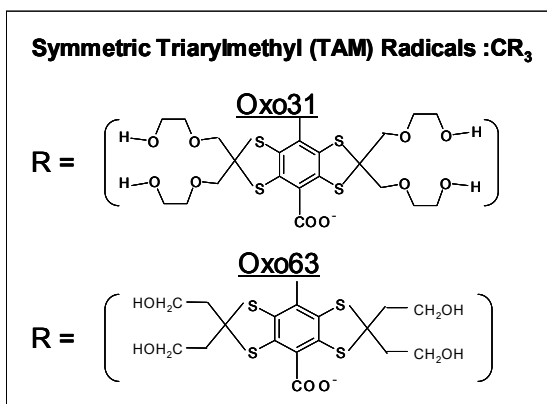

Fig.7   The structure of two symmetrical triarylmethyl derivatives namely Oxo31 and Oxo63 used in Overhauser enhanced MRI and pulsed EPR. They g=have narrow line widths, relxatione times in the range 5-6 μs and oxygen-dependent line wdiths

3.4 In vivo probes based on triarylmethyl(TAM)

Although stable, water-soluble, non-toxic paramagnetic compounds are quite suitable for in vivo EPR spectroscopy and imaging, in order to perform time-domain spectroscopy and imaging (pulsed EPR), we need to have paramagnetic agents that will have sufficiently long relaxation times by way of very narrow line width. Most nitroxides have line width on the order of a Gauss corresponding transverse relaxation times on the order of 100 ns which is too short. Fully deuterated nitroxides such as perdeuterated tempol derivatives have line widths in the range 100-250 mG.

Recently Nycomed Innovations in Sweden have synthesized a series of narrow-line spin probes based on the triarylmethyl(TAM) motif mainly for the purpose of performing dynamic nuclear polarization, DNP (also known as Overhauser enhancement) based NMR spectroscopy and imaging[88-90]. These compound have line widths even narrower than the deuterated nitroxides, and are water soluble, non-troxic, and some od these compounds have sufficiently long half-life that one can perform in vivo Overhauser enhance MR imaging (OMRI) and spectroscopy. The detailed magnetic properties of these compounds have been described elsewhere[88-90]. Two of the compounds used in OMRI experiments are given in Fig.7. Although the intrinsic line widths of these compounds are on the order of 50 mG, due to unresolved hyperfine coupling, the apparent line width could be upto 200 mG when measured by low frequency EPR. These compounds are ideal for highly enhanced spectroscopic investigations of ^{13}C in metabolites which, under normal conditions, due to very low abundance and low magnetic moments, give very poor signals. In the same token, these TAM based radicals are ideal for performing oxymetric MR imaging at very low fields on the order of 10 mT. The

principle of Overhauser oxymetry in a nutshell is as follws. When a paramagnetic substance is saturated under EPR conditions, the electrons transfer their magnetization to their dipolar coupled nuclear neighbours (for example solvent water protons) resulting in a net polarization that is proportional to the ratio of the electronic to nuclear magnetic moment. For protons, this is around 330, such that an MR image taken at 10mT with DNP, will have SNR equivalent to MRI taken 3T. This immediately opens up a lot of possibilities of functional imaging. This is because, the efficiency of DNP depends on the degree of saturation, which for a given MW/RF power depends on the linewidth of the spin probe. Fortunately, the TAM based radicals have a reasonable oxygen relaxivity. One can use this to perform DNP MRF imaging with different power levels and derive quantitative information on the levels of tissue oxygenation[40].(Fig.8)

The ultra narrow line widths of TAM radicals make them ideal spin probes for high resolution EPR imaging both in the CW and time-domain imaging mode. We have extensively used the TAM radicals to develop our time-domain in vivo EPR imaging instrumentation[40, 47] and now routinely perform oxymetric imaging. We use a pure phase-encoding mode of imaging known as the single point imaging[40]. Our automated pulsed EPR imaging system, evolved over a decade of developments, uses state-of-the-art data acquisition system, incorporating very fast gradient-switching and excellent isolation between transmit and receive sections. We can perform three dimensional imaging and spatially oxymetry with 1 mm resolution and distinguish pO_2 differing by ± 5 mm of Hg. Representative examples of 3D imaging and
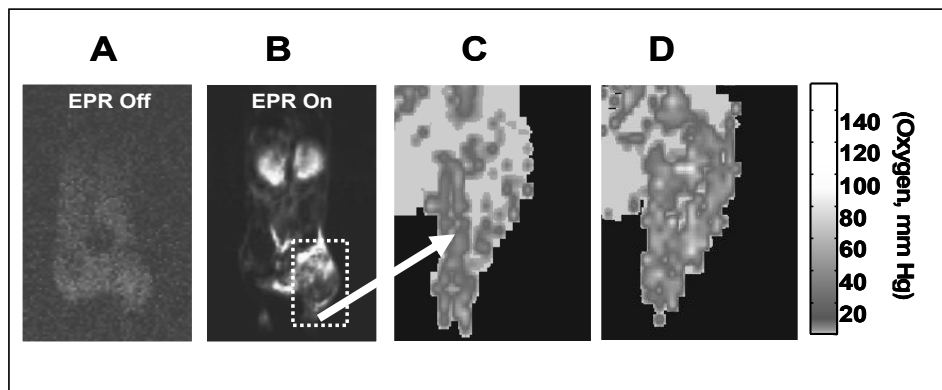

Fig.8 A. The proton MRI iamge of a C3H mouse with SCC tumor on the right leg measured at very low field (250 MHz) with natural polarization. B. the same mouse measured after injection of Oxo63 followed by overhauser enhancement. C. Oxygen image derived from Overhauser imaging method showing the heterogeneous distribution of hypoxic zones in the tumor when the mouse was breathing ambient air. D.The marked increase in the oxygen seen when the mouse was allowed to breathe Carbogen (95% O_2 and 5 % CO_2)

oxymetry in mouse SCC tumor are given in Figs.9 &10. The figure caption details the measurement conditions. We have also carried out tumor oxygenation measurements when the mouse is allowed switch from breathing ambient air to Carbogen and found a distinct increase in oxygenation[47]. Such studies will help schedule fractionated radiation in the efficient treatment of tumors by radiation or chemotherapeutic agents.

Halpern et al. have used one of the TAM derivatives in the measurement of 4-dimensional spectral spatial imaging of mouse tumors using the CWEPR methodology at 250 MHz[91].. They also investigated the effect of Cabogen breathing on tumor oxygenation and were able to corroborate the EPR oxymetry results with that of BOLD MRI performed on the same mouse[92]. Liu et al. have employed the per-deuterated nitroxide 3-carboxy-2,2,5,5-tetramethylpyrrolidine-1-oxyl (PCA)*(this nitroxide can cross the blood-brain barrier) in the in vivo measurement of oxidative stress in stroke models of rat brain by EPR[93]. Kuppusamy et al. have employed a novel, polynitroxylated derivative of human serum albumin that is shown to be capable of reoxidizing the hydroxylamine back to nitroxide *in* vivo. Polynitroxyl-albumin (PNA) is shown to be effective in maintaining the signal intensity of the nitroxide 4-hydroxy-2,2,6,6-tetramethylpiperidine-1-oxyl (TEMPOL or TPL) in the ischemic isolated rat heart, allowing the acquisition of high-resolution three-dimensional (3D) EPR images of the heart throughout a prolonged 2.5 hour period of global cardiac ischemia[94]. Literally hundreds of nitroxides have been synthesized with tailored properties to address specific bioactivity and it is envisaged that EPR

spectroscopy & imaging will develop to be an important tool to interrogate a variety of pathophysiological conditions in animal models.
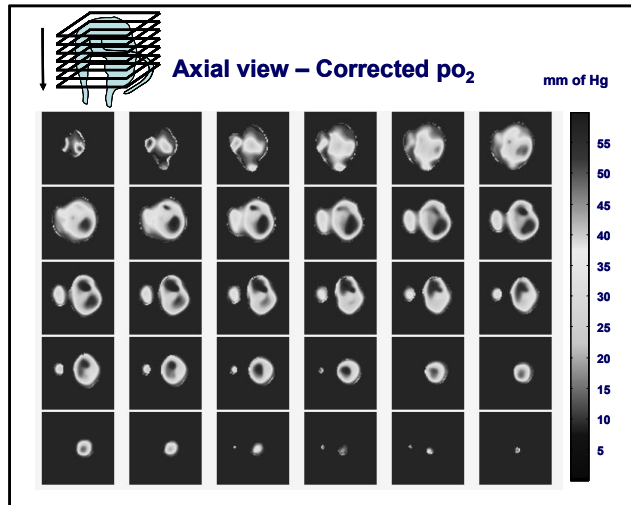

Fig. 9 Axial slices of pO$_2$ (alternate 0.6 mm slices) derived from a multi-gradient 3D SPI image. pO$_2$ maps were derived from the pixelwise decay of signals as modified by the in vivo oxygen concentration The greatly reduced pO2 in the tumor leg, the presence of the hypoxic cores, and the heterogeneity in the tumor oxygen distribution, etc. can be seen.
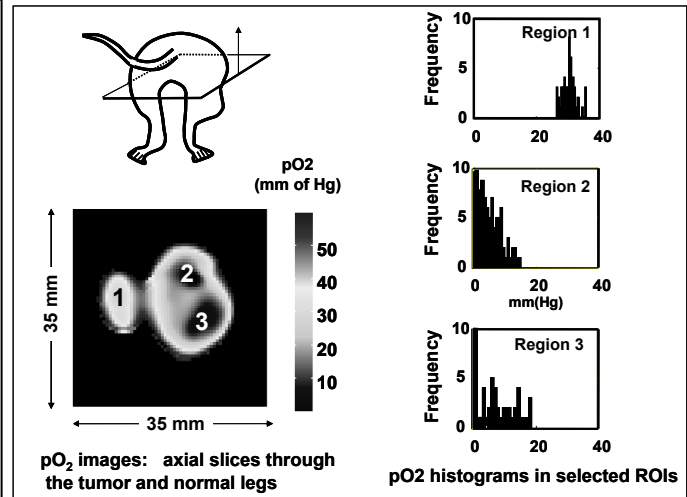
Fig. 10 **Left:**An axial oxymetric slice passing thorough the normal and tumor legs derived from 3D multi-gradient SPI images. The higher pO2 in the normal leg and the relative lower pO$_2$ and regions of near-zero pO$_2$ (hypoxic zones) in the tumor leg can be clearly discerned. **Right:**The three regions 1,2 and 3 shown are used to look at the oxygen histograms in the two legs. Regions 2 and 3 from inside the tumor shows region of near-zero pO$_2$.

3.5 Spin probes for in vivo detecting nitric oxide by EPR

Nitric oxide is a very important signaling molecule in the mammalian system. The measurement of nitric oxide (NO). In the body, nitric oxide (the 'endothelium-derived relaxing factor', or 'EDRF') is synthesized from arginine and oxygen by various nitric oxide synthase enzymes (NOS) and by sequential reduction of inorganic nitrate. Nitric oxide can contribute to reperfusion injury. when excessive nitric oxide produced during reperfusion. The ability to detect NO non-invasively in living animals or excised organs has great potential using specialized electron paramagnetic resonance (EPR) methods. Although NO is paramagnetic, it cannot be observed directly unless it is complexed with ferrous iron-dithiocarbamate ligand spin trap complexes. Despite the minimally invasive nature of the technique, highly sensitive localized concentrations of NO may be observed ("trapped") *in vivo* by both L-band EPR and magnetic resonance imaging[95]. The spin traps used are Iron(II)diethyldithiocarbomate (hydrophobic) and Iron(II)-*N*-Methyl-D-glucamine dithiocarbamate (hydrophilic) Complexes. These iron complexes are four co-ordiante planar diamagnetic compounds which have a great affinity for trapping NO. As soon as the NO is trapped, an electron get transferred from the Fe(II) to the NO ligand so that, formally, Fe(II) becomes oxidized to Fe(III) and NO gets reduced to NO$^-$ The di-thiocarbamate ligands provide a strong ligand field thereby keeping the Fe(III) in the low spin state (S=1/2) which gives a room temperature spectrum consisting of a triplet hyperfine pattern from the attached nitrogen of the NO ligand. Several EPR spectroscopic and imaging experiments have been carried out to explore in vivo generation of NO and their estimation[96-98] Excessive amounts of NO in vivo can cause or contribute to vascular shock, stroke, diabetes, neurodegeneration, arthritis and chronic inflammation. EPR spectroscopy can also be conducted ex-vivo to interrogate NO production. Komaro and Lai[99] have reported the study of NO production in lipopolysaccharide (LPS) challenged mouse by EPR. Normal or LPS-treated mice were injected subcutaneously with N-methyl-D-glucamine dithiocarbamate-ferrous iron, [(MGD)2/Fe], which binds to NO and forms a water-soluble [(MGD)2/Fe-NO] complex. At 2 h after injection of the [(MGD)2/Fe] complex, a three-line EPR signal characteristic of the [(MGD)2/Fe-NO] complex was detected in the urine of either normal or LPS-treated mice. It is estimated that the concentrations of the

[(MGD)2/Fe-NO] complex in normal and LPS-treated mouse urine were 1.3 and 35 μM, respectively. This 25-fold increase in NO levels in the LPS-treated mouse urine provides the direct evidence that LPS challenge induces the overproduction of NO in mice. Fuji et al[95] confirmed the production of NO by the LPS challenge in mice in an in vivo L-Bnad investigation. Several in vivo EPR experiments have been reported by others for the detection NO by complexation with the Iron dithiocarnamate complexes.

4. SUMMARY AND PROSPECTS

EPR imaging in vivo is anyoung and upcoming field, and we have only seen some of the possible applications of in vivo EPR in such areas as imaging, tissue oxygenation, redox status, pharmacokinetics etc. Commercially only recently L-Band EPR imaging machines are becoming available. With the availability of TAM-based narrow line free radicals, the pulsed EPR imaging and spectroscopy have really become very effective. New and novel paramagnetic synthetic spin probes will definitely increase the scope and applications of functional EPR imaging. We have not paid any attention to the vast number of applications of EPR spectroscopy to dermatology, wound healing, etc. Just as Gadolinium based contrast agents, and super paramagnetic iron oxide (SPIO) have revolutionized the application of MRI to generate a host of functional information, synthesis of new redox sensitive, biochemically specific spin probes and spin-trapping agents will further expand the potential of EPR imaging and spectroscopy in helping us to understand a little more about the life processes.

5. REFRENCES

1   C. T. W. Moonen, P. A. Bandettini, G. K. Aquirre, and H. P. Heilman, *Functional MRI*. Springer Verlag: New York, 1999.
2   S. Ogawa, D. W. Tank, R. Menon, J. M. Ellerman, S. G. Kim, H. Merkle, and K. Ugurbil, "Intrinsic signal changes accompanying sensory stimulation -functional brain mapping with magnetic resonance imaging" *Proc. Natl. Acad. Sc.i USA*. 89, 5951-5955 (1992).
3   P. C. M. vanZijl, S. M. Eleff, J. A. Ulatowsjki, J. M. E. Ojal, A. M. Ulu, R. J. Traystman, and R. A. Kauppinen, " Quantitative assessment of blood flow, blood volume and blood oxygenation effects in functional magnetic resonance imaging" *Nature Medicne* 4, 159-167 (1998).
4   E. Zavoisky, "Spin-magnetic resonance in paramagnetics" *Journal of Phyiscs E* 9, 245-249 (1945).
5   F. Bloch, W. W. Hansen, and H. E. Packard, "Nuclear Induction" *Physical Review* 69, 127-131 (1946).
6   E. H. Purcell, H. C. Torrey, and R. V. Pound, "Resonance absorption by nuclear moments in solid" *Physical Review* 69, 37-38 (1946).
7   M. Gomberg, *J. Amer. Chem. Soc.* 69, 2921-2925 (1947).
8   E. Scarlata, A. Descalzo, M. Insani, L. Rossetti, and N. Pensel, "Lipid peroxidation, oxidative stress, protein oxidation and antioxidant capacity during skeletal muscle regeneration in vivo" *Free Radical Biology and Medicine* 36, S84-S84 (2004).
9   H. Rubbo, R. Radi, M. Trujillo, R. Telleri, B. Kalyanaraman, S. Barnes, M. Kirk, and B. A. Freeman, "Nitric-Oxide Regulation of Superoxide and Peroxynitrite-Dependent Lipid-Peroxidation - Formation of Novel Nitrogen-Containing Oxidized Lipid Derivatives" *Journal of Biological Chemistry* 269, (42), 26066-26075 (1994).
10   V. Renault, L. E. Thornell, G. Butler-Browne, and V. Mouly, "Human skeletal muscle satellite cells: aging, oxidative stress and the mitotic clock" *Experimental Gerontology* 37, (10-11), 1229-1236 (2002).
11   R. S. Sohal, "The Free-Radical Hypothesis of Aging - an Appraisal of the Current Status" *Aging-Clinical and Experimental Research* 5, (1), 3-17 (1993).
12   L. J. Berliner, *In Vivo EPR (ESR)*. Kluwer Academic: New York, 2003; Vol. 18.
13   E. G. Janzen, and B. Blackburn, J., "Detection and identification of short-lived free radicals by electron spin resonance trapping technique" *J. Amer. Chem. Soc.* 90, 5909-5910 (1968).
14   B. Bodis, O. Karadi, I. Szabo, P. Nemeth, J. Belagyi, and G. Mozsik, "Evidence for the involvement of oxygen free radicals in the ethanol-induced late cellular injury in mouse myeloma cells" *Journal of Physiology-Paris* 94, (1), 67-70 (2000).

15   D. A. Stoyanovsky, Z. Melnikov, and A. I. Cederbaum, "ESR and HPLC analysis of the interaction of hydroxyl radical with DMSO: Rapid reduction and quantification of POBN and PBN nitroxides" *Analytical Chemistry* 71, (3), 715-721 (1999).

16   N. Vrbjar, S. Zollner, R. E. Haseloff, M. Pissarek, and I. E. Blasig, "PBN spin trapping of free radicals in the reperfusion-injured heart. Limitations for pharmacological investigations" *Molecular and Cellular Biochemistry* 186, (1-2), 107-115 (1998).

17   L. J. Berliner, and J. Reuben, *Spin labeling: Theory and applications*. Plenum: Nwe York, 1989; Vol. 8.

18   K. Matsuda, M. T. Stone, and J. S. Moore, "Helical pitch of m-phenylene ethynylene foldamers by double spin labeling" *Journal of the American Chemical Society* 124, (40), 11836-11837 (2002).

19   V. Monaco, F. Formaggio, M. Crisma, C. Toniolo, P. Hanson, G. Millhauser, C. George, J. R. Deschamps, and J. L. Flippen-Anderson, "Determining the occurrence of a 3(10)-helix and an alpha-helix in two different segments of a lipopeptaibol antibiotic using TOAC, a nitroxide spin-labeled C-alpha-tetrasubstituted alpha-amino acid" *Bioorganic & Medicinal Chemistry* 7, (1), 119-131 (1999).

20   P. R. Proctor, *Free radicals and human disease. In: CRC Handbook of Free Radicals andAntioxidants in Biomedicine.* . CRC Press: Boca Raton, Fla., 1989.

21   B. Haliwell, and J. Gutteridge, *Free Radicals in Biology and Medicine* Oxford University Press: New York, 1999.

22   R. K. Nesbet, "Molecular Model of the Heisenberg Exchange Interaction " *Phys. Rev.* 122, 1497-1508

23   H. M. Swartz, and R. B. Clarkson, "The measurement of oxygen in vivo using EPR techniques" *Phys Med Biol* 43, 1957-1975 (1998).

24   G. Ilangovan, J. L. Zweier, and P. Kuppusamy, "Electrochemical preparation and EPR studies of lithium phthalocyanine. Part 2: Particle-size-dependent line broadening by molecular oxygen and its implications as an oximetry probe" *Journal of Physical Chemistry B* 104, (40), 9404-9410 (2000).

25   G. Ilangovan, J. L. Zweier, and P. Kuppusamy, "Electrochemical preparation and EPR studies of lithium phthalocyanine: Evaluation of the nucleation and growth mechanism and evidence for potential-dependent phase formation" *Journal of Physical Chemistry B* 104, (17), 4047-4059 (2000).

26   J. A. Brivati, A. D. Stevens, and M. C. R. Symons, "A radiofrequency ESR spectrometer for in vivo imaging" *Journal of magnetic resonance* 92, 480-489 (1991).

27   H. J. Halpern, and M. K. Bowman, *Low frequency EPR spectrometers: MHz range*. CRC Press: Boca Raton, 1991.

28   J. Koscielniak, N. Devasahayam, M. S. Moni, P. Kuppusamy, K. Yamada, J. B. Mitchell, M. C. Krishna, and S. Subramanian, "300 MHz continuous wave electron paramagnetic resonance spectrometer for small animal in vivo imaging" *Review of Scientific Instruments* 71, (11), 4273-4281 (2000).

29   M. Alecci, J. A. Brivati, G. Placidi, and A. Sotgiu, "A radiofrequency (220-MHz) Fourier transform EPR spectrometer" *Journal of Magnetic Resonance* 130, (2), 272-280 (1998).

30   R. Murugesan, M. Afeworki, J. A. Cook, N. Devasahayam, R. Tschudin, J. B. Mitchell, S. Subramanian, and M. C. Krishna, "A broadband pulsed radio frequency electron paramagnetic resonance spectrometer for biological applications" *Review of Scientific Instruments* 69, (4), 1869-1876 (1998).

31   R. W. Quine, G. W. Rinard, S. S. Eaton, and G. R. Eaton, "A pulsed and continuous wave 250 MHz electron paramagnetic resonance spectrometer" *Concepts in Magnetic Reosnance (Magnetic Resonance Engineering)* 15, (1), 59-91 (2002).

32   S. Subramanian, J. B. Mitchell, and M. C. Krishna, in *Biological Magnetic Resonance*, ed. Berliner, L. J., Kluwer Academic: New York, 2003; Vol. 18, pp 153-197.

33   G. R. Eaton, S. E. Eaton, and K. Ohno, *EPR imaging and in vivo EPR*. CRC Press: Boca Raton, 1991.

34   P. Kuppusamy, P. H. Wang, M. Chzhan, and J. L. Zweier, "High resolution electron paramagnetic resonance imaging of biological samples with a single line paramagnetic label" *Magnetic Resonance in Medicine* 37, (4), 479-483 (1997).

35   P. C. Lauterbur, "Image Formation by Induced Local Interactions: Examples Employing Nuclear Magnetic Resonance" *Nature* 242, 190-191 (1973).

36   B. Balcom, S. D. Beyea, D. P. Green, R. L. Armstrong, and T. W. Bremner, "Single-Point Ramped Imaging with T1 Enhancement (SPRITE)" *J Magn Reson A* 123, 131-134 (1996).

37   S. Emid, and J. H. N. Creyghton, "High-resolution NMR imaging in solids" *Physica* 128B, 81-83 (1985).

38   S. Gravina, and D. G. Cory, "Sensitivity and resolution of constant-time imaging" *Journal of Magnetic Resonance B* 104, 53-61 (1994).

39   M. Halse, J. Rioux, S. Romanzetti, J. Kaffanke, B. MacMillan, I. Mastikhin, N. J. Shah, E. Aubanel, and B. J. Balcom, "Centric scan SPRITE magnetic resonance imaging: optimization of SNR, resolution, and relaxation time mapping" *J. Magn. Reson.* 169, 102-117 (2004).

40   M. C. Krishna, S. English, K. Yamada, J. Yoo, R. Murugesan, N. Devasahayam, J. A. Cook, K. Golman, J. H. Ardenkjaer-Larsen, S. Subramanian, and J. B. Mitchell, "Overhauser enhanced magnetic resonance imaging for tumor oximetry: Coregistration of tumor anatomy and tissue oxygen concentration" *Proceedings of the National Academy of Sciences of the United States of America* 99, (4), 2216-2221 (2002).

41   G. R. Eaton, S. S. Eaton, and M. M. Maltempo, "3 Approaches to Spectral Spatial Epr Imaging" *Applied Radiation and Isotopes* 40, (10-12), 1227-1231 (1989).

42   M. Elas, B. B. Williams, A. Parasca, C. Mialer, C. A. Pelizzari, M. A. Lewis, J. N. River, G. S. Karczmar, E. D. Barth, and H. J. Halpern, "Quantitaive tumor oximetric images from 4D electron paramagnetic resonance iamging (EPRI): methodology and comparison with blood oxygen level-dependent (BOLD) MRI" *Magnetic Resonance in Medicine* 49, (4), 682-691 (2003).

43   P. Kuppusamy, M. Chzhan, K. Vij, M. Shteynbuk, D. J. Lefer, E. Giannella, and J. L. Zweier, "3-Dimensional Spectral Spatial Epr Imaging of Free-Radicals in the Heart - a Technique for Imaging Tissue Metabolism and Oxygenation" *Proceedings of the National Academy of Sciences of the United States of America* 91, (8), 3388-3392 (1994).

44   M. M. Maltempo, "Differentiation of spectral and spatial components in EPR imaging using 2-D image reconstruction algorithms" *Journal of Magnetic Resonance* 69, 156-163 (1986).

45   M. M. Maltempo, S. S. Eaton, and G. R. Eaton, "Spectral-spatial two dimensional EPR imaging" *Journal of Magnetic Resonance* 72, 449-455. (1987).

46   S. D. Balcom, S. D. Beyea, D. P. Green, R. L. Armstrong, and T. W. Brenner, "Imaging of heterogeneous materials with a turbo spin echo single-point imaging technique" *Journal of magnetic Resonance* 144, 255-265 (1996).

47   S. Subramanian, K. I. Matsumoto, J. B. Mitchell, and M. C. Krishna, "Radio frequency continuous-wave and time-domain EPR imaging and Overhauser-enhanced magnetic resonance imaging of small animals: instrumental developments and comparison of relative merits for functional imaging" *Nmr in Biomedicine* 17, 263-294 (2004).

48   J. Uebersfeld, and E. Erb, "Resonance Paramagnetique Dans Les Charbons - Effets De Surface" *Journal De Physique Et Le Radium* 17, (5), 452-453 (1956).

49   J. Uebersfeld, and E. Erb, "Saturation Et Temps De Relaxation Dans La Resonance Paramagnetique Electronique Des Charbons De Sucre" *Comptes Rendus Hebdomadaires Des Seances De L Academie Des Sciences* 243, (25), 2043-2044 (1956).

50   J. Uebersfeld, and E. Erb, "Resonance Paramagnetique Des Charbons - Detection Dun Radical Libre Instable a Lair" *Journal De Physique Et Le Radium* 16, (4), 340-340 (1955).

51   R. B. Clarkson, W. Wang, D. R. Brown, H. C. Crookham, and R. L. Belford, "Electron Magnetic-Resonance of Standard Coal Samples at Multiple Microwave-Frequencies" *Advances in Chemistry Series*, (229), 507-528 (1993).

52   B. Gallez, R. Debuyst, F. Dejehet, K. J. Liu, T. Walczak, F. Goda, R. Demeure, H. Taper, and H. M. Swartz, "Small particles of fusinite and carbohydrate chars coated with aqueous soluble polymers: Preparation and applications for in vivo EPR oximetry" *Magnetic Resonance in Medicine* 40, (1), 152-159 (1998).

53   H. M. Swartz, and T. Walczak, "Developing in vivo EPR oximetry for clinical use" *Advances in Experimental Medical Biology* 454, 243-252 (1998).

54   N. Vahidi, R. B. Clarkson, K. J. Liu, S. W. Norby, M. Wu, and H. M. Swartz, "In-Vivo and in-Vitro Epr Oximetry with Fusinite - a New Coal-Derived, Particulate Epr Probe" *Magnetic Resonance in Medicine* 31, (2), 139-146 (1994).

55   F. Goda, K. J. Liu, T. Walczak, J. A. Ohara, J. J. Jiang, and H. M. Swartz, "In-Vivo Oximetry Using Epr and India Ink" *Magnetic Resonance in Medicine* 33, (2), 237-245 (1995).

56   J. A. OHara, F. Goda, J. F. Dunn, and H. M. Swartz, "Potential for EPR oximetry to guide treatment planning for tumors" *Oxygen Transport to Tissue Xviii* 411, 233-242 (1997).

57   K. Mader, H. M. Swartz, R. Stosser, and H. H. Borchert, "The Application of Epr Spectroscopy in the Field of Pharmacy" *Pharmazie* 49, (2-3), 97-101 (1994).

58   M. Afeworki, N. R. Miller, N. Devasahayam, J. Cook, J. B. Mitchell, S. Subramanian, and M. C. Krishna, "Preparation and EPR studies of lithium phthalocyanine radical as an oxymetric probe" *Free Radical Biology and Medicine* 25, (1), 72-78 (1998).

59   G. Ilangovan, H. Q. Li, J. L. Zweier, and P. Kuppusamy, "Electrochemical preparation and EPR studies of lithium phthalocyanine. 3. Measurements of oxygen concentration in tissues and biochemical reactions" *Journal of Physical Chemistry B* 105, (22), 5323-5330 (2001).

60   K. J. Liu, P. Gast, M. Moussavi, S. W. Norby, N. Vahidi, T. Walzak, M. Wu, and H. M. Swartz, "Lithium phthalocyanine: a probe for electron paramagnetic resonance oximetry in viable biologic systems" *Processings of the National Academy of Sciences (USA)* 90, 5438-5442. (1993).

61   A. Matsumoto, S. Matsumoto, A. L. Sowers, J. W. Koscielniak, N. J. Trigg, P. Kuppusamy, J. B. Mitchell, S. Subramanian, M. C. Krishna, and K. Matsumoto, "Absolute oxygen tension (pO(2)) muscle tissue as determined by in murine fatty and EPR" *Magnetic Resonance in Medicine* 54, (6), 1530-1535 (2005).

62   A. Matsumoto, S. Matsumoto, A. Sowers, P. Kuppusomy, J. Mitchell, S. Subramanian, M. Krishna, and K. I. Matsumoto, "Assessment of absolute oxygen concentration in normal mouse tissues using low field magnetic resonance spectroscopy" *Free Radical Biology and Medicine* 37, S184-S184 (2004).

63   A. Manivannan, and H. Yanagi, "Synthesis and spectral properties of lithium naphthalocyanine: A novel EPR oximetry probe" *Chemistry Letters*, (6), 568-569 (2001).

64   A. Manivannan, H. Yanagi, G. Ilangovan, and P. Kuppusamy, "Lithium naphthalocyanine as a new molecular radical probe for electron paramagnetic resonance oximetry" *Journal of Magnetism and Magnetic Materials* 233, (3), L131-L135 (2001).

65   R. P. Pandian, N. L. Parinandi, G. Ilangovan, J. L. Zweier, and P. Kuppusamy, "Novel particulate spin probe for targeted determination of oxygen in cells and tissues" *Free Radical Biology and Medicine* 35, (9), 1138-1148 (2003).

66   R. P. Pandian, Y. I. Kim, P. M. Woodward, J. L. Zweier, P. T. Manoharan, and P. Kuppusamy, "The open molecular framework of paramagnetic lithium octabutoxynaphthalocyanine: implications for the detection of oxygen and nitric oxide using EPR spectroscopy" *Journal of Materials Chemistry* 16, (36), 3609-3618 (2006).

67   C. S. Lai, L. E. Hopwood, J. S. Hyde, and S. Lukiewicz, "ESR stuies of O2 uptake by Chinese hamster ovary cells during the cell cycle" *Proc.Nadl.Acad.Sci.USA1166-1170.* 79, 1166-1170 (1982).

68   H. M. Swartz, "Use of nitroxides to measure redox metabolism in cells and tissues" *J.Chem.Soc.FaradayTrans.* 183, 191-202 (1987).

69   J. Dobrucki, F. W.Demsar, T. Walczak, R. K. Woods, G. Bacic, and H. M. Swartz, *Br.J.Cancer* 61, 221-224 (1990).

70   J. Towell, and B. Kalyanaraman, *Anal.Biochem.* 196, 111-119 (1991).

71   H. M. Swartz, "Principles of the Metabolism of Nitroxides and Their Implications for Spin Trapping" *Free Radical Research Communications* 9, (3-6), 399-405 (1990).

72   S. Belkin, R. J. Mehlhorn, K. Hideg, O. Hankovsky, and L. Packer, "Reduction and Destruction Rates of Nitroxide Spin Probes" *Archives of Biochemistry and Biophysics* 256, (1), 232-243 (1987).

73   A. Samuni, C. M. Krishna, P. Riesz, E. Finkelstein, and A. Russo, "A Novel Metal-Free Low-Molecular Weight Superoxide-Dismutase Mimic" *Journal of Biological Chemistry* 263, (34), 17921-17924 (1988).

74   J. B. Mitchell, W. Degraff, D. Kaufman, M. C. Krishna, A. Samuni, E. Finkelstein, M. S. Ahn, S. M. Hahn, J. Gamson, and A. Russo, "Inhibition of Oxygen-Dependent Radiation-Induced Damage by the Nitroxide Superoxide-Dismutase Mimic, Tempol" *Archives of Biochemistry and Biophysics* 289, (1), 62-70 (1991).

75   D. Gelvan, P. Saltman, and S. R. Powell, "Cardiac Reperfusion Damage Prevented by a Nitroxide Free-Radical" *Proceedings of the National Academy of Sciences of the United States of America* 88, (11), 4680-4684 (1991).

76   U. A. Nilsson, L. I. Olsson, G. Carlin, and A. C. Bylundfellenius, "Inhibition of Lipid-Peroxidation by Spin Labels - Relationships between Structure and Function" *Journal of Biological Chemistry* 264, (19), 11131-11135 (1989).

77   J. Chateauneuf, J. Lusztyk, and K. U. Ingold, "Absolute Rate Constants for the Reactions of Some Carbon-Centered Radicals with 2,2,6,6-Tetramethylpiperidine-N-Oxyl" *Journal of Organic Chemistry* 53, (8), 1629-1632 (1988).

78   F. Q. Schafer, and G. R. Buettner, "Redox environment of the cell as viewed through the redox state of the glutathione disulfide/glutathione couple" *Free Radical Biology and Medicine* 30, (11), 1191-1212 (2001).

79 A. Russo, J. Carmichael, N. Friedman, W. Degraff, Z. Tochner, E. Glatstein, and J. B. Mitchell, "The Roles of Intracellular Glutathione in Antineoplastic Chemotherapy" *International Journal of Radiation Oncology Biology Physics* 12, (8), 1347-1354 (1986).

80 N. Y. Yu, and J. M. Brown, "Depletion of Glutathione Invivo as a Method of Improving the Therapeutic Ratio of Misonidazole and Sr-2508" *International Journal of Radiation Oncology Biology Physics* 10, (8), 1265-1269 (1984).

81 M. C. Krishna, D. A. Grahame, A. Samuni, J. B. Mitchell, and A. Russo, "Oxoammonium Cation Intermediate in the Nitroxide-Catalyzed Dismutation of Superoxide" *Proceedings of the National Academy of Sciences of the United States of America* 89, (12), 5537-5541 (1992).

82 G. Ilangovan, H. Q. Li, J. L. Zweier, M. C. Krishna, J. B. Mitchell, and P. Kuppusamy, "In vivo measurement of regional oxygenation and Imaging of redox status in RIF-1 murine tumor: Effect of carbogen-breathing" *Magnetic Resonance in Medicine* 48, (4), 723-730 (2002).

83 G. L. He, Y. M. Deng, H. H. Li, P. Kuppusamy, and J. L. Zweier, "EPR/NMR co-imaging for anatomic registration of free-radical images" *Magnetic Resonance in Medicine* 47, (3), 571-578 (2002).

84 J. B. Mitchell, M. C. Krishna, P. Kuppusamy, J. A. Cook, and A. Russo, "Protection against oxidative stress by nitroxides" *Experimental Biology and Medicine* 226, (7), 620-621 (2001).

85 P. Kuppusamy, M. Chzhan, P. H. Wang, and J. L. Zweier, "3D gated EPR imaging of the beating heart" *Biophysical Journal* 70, (2), Su409-Su409 (1996).

86 A. Tomasi, and E. Albano et al, in *Medical, Biomedical and Chemical Aspects of Free Radicals* eds. Hayashi, O.; Niki, E.; Kon, M., 1988.

87 K. Mader, and B. Gallez, "Pharmaceutical applications of in vivo EPR" *Biological Magnetic Resonance* 18, 515-545 (2003).

88 J. H. Ardenkjaer-Larsen, I. Laursen, I. Leunbach, G. Ehnholm, L. G. Wistrand, J. S. Petersson, and K. Golman, "EPR and DNP properties of certain novel single electron contrast agents intended for oximetric imaging" *Journal of Magnetic Resonance* 133, (1), 1-12 (1998).

89 K. Golman, I. Leunbach, J. S. Petersson, D. Holz, and J. Overweg, "Overhauser-enhanced MRI" *Academic Radiology* 9, S104-S108 (2002).

90 K. Golman, J. S. Petersson, J. H. Ardenkjaer-Larsen, I. Leunbach, L. G. Wistrand, G. Ehnholm, and K. C. Liu, "Dynamic in vivo oxymetry using Overhauser enhanced MR imaging" *Journal of Magnetic Resonance Imaging* 12, (6), 929-938 (2000).

91 M. Elas, B. B. Williams, A. Parasca, C. Mailer, P. C. A., M. A. Lewis, J. N. River, G. S. Karczmar, E. D. Barth, and H. J. Halpern, "Quantitative tumor oxymetric images from 4D electron paramagnetic resonance imaging (EPRI): Methodology and comparison with blood oxygen level-dependent (BOLD) MRI" *Magnetic Resonance in Medicine* 49, 682-691 (2003).

92 B. B. Williams, H. al Hallaq, G. V. R. Chandramouli, E. D. Barth, J. N. Rivers, M. Lewis, V. E. Galtsev, G. S. Karczmar, and H. J. Halpern, "Imaging spin probe distribution in the tumor of a living mouse with 250 MHz EPR: Correlation with BOLD MRI" *Magnetic Resonance in Medicine* 47, (4), 634-638 (2002).

93 S. M. Liu, G. S. Timmins, H. L. Shi, C. M. Gasparovic, and K. J. Liu, "Application of in vivo EPR in brain research: monitoring tissue oxygenation, blood flow, and oxidative stress" *Nmr in Biomedicine* 17, 327-328 (2004).

94 P. Kuppusamy, H. Q. Li, G. Ilangovan, A. J. Cardounel, J. L. Zweier, K. Yamada, M. C. Krishna, and J. B. Mitchell, "Noninvasive imaging of tumor redox status and its modification by tissue glutathione levels" *Cancer Research* 62, (1), 307-312 (2002).

95 H. Fujii, and L. J. Berliner, "Nitric oxide: prospects and perspectives of in vivo detection by L-band EPR spectroscopy" *Physics in Medicine and Biology* 43, (7), 1949-56 (1998).

96 A. M. Komarov, "In vivo on-line detection of NO distribution in endotoxin-treated mice by L-band ESR" *Cellular and Molecular Biology* 46, (8), 1329-1336 (2000).

97 A. M. Komarov, "In vivo detection of nitric oxide distribution in mice" *Molecular and Cellular Biochemistry* 234, (1), 387-392 (2002).

98 A. M. Komarov, J. Joseph, and C. S. Lai, "In-Vivo Pharmacokinetics of Nitroxides in Mice" *Biochemical and Biophysical Research Communications* 201, (2), 1035-1042 (1994).

99 A. M. Komarov, and C. S. Lai, "Detection of nitric oxide production in mice by spin-trapping electron paramagnetic resonance spectroscopy" *Biochim. Biophys. Acta.* 1272, 29-36 (1995).